Вісник ХНУ, серія «Фізика», вип. 25, 2016. с. 26-29

PACS numbers: 42.15.-i; 42.25.-p; 42.50.Ct; 42.50.Wk; 42.62.Fi; 42.65.-k
УДК 535.016; 535.1; 535.318; 535.321.9; 535.324.2; 535.39; 535.434

Stimulated Doppler effect on the surface of a gas bubble thermocapillary trapped by a laser in an absorbing liquid

V.I. Lymar, N.A. Kazachkova, O.I. Kofman, N.V. Slabunova, N.A. Luzan

V.N. Karazin Kharkiv National University, Svobody Sq., 4, Kharkiv, 61022, Ukraine
lymar@univer.kharkov.ua

A possibility to control the gas bubble size in an absorbing liquid through the laser thermo-capillary trapping has been demonstrated. The coarse structure of the observed interference patterns in reflected and transmitted lights are explained qualitatively within the framework of a two-ray approach. The movement of interference fringes can be treated as manifestation of the Doppler effect because of the moving bubble walls. The method to measure the relative refractive index value for moving contiguous media by means of the Doppler shifts ratio measurement has been proposed. There is a two times discrepancy between Doppler shifts ratio value predicted theoretically and measured in the experiment. It is following from a special stimulated character of the Doppler effect at experimentally realized non-equilibrium thermodynamic conditions, that are imposed by the laser light field.
Keyword: thermocapillary trap; gas bubble; laser beam scattering; interference pattern; refractive index; Doppler effect.

Продемонстровано можливість контролю та управління розміром газової бульбашки, яка знаходиться у поглинаючій світло рідині та захоплена у лазерну термокапілярну пастку. Груба структура інтерференційних картин, що спостерігаються у відбитому та пройденому світлі, пояснюється якісно в рамках двопроменевого наближення. Рух інтерференційних смуг можна розглядати як прояв ефекту Доплера на рухомих стінках бульбашки. Запропоновано метод визначення відносного показника заломлення двох суміжних середовищ з рухомою границею розділу між ними через вимірювання відношення доплерівських зсувів частот. Наявне двократне розходження у значеннях цього відношення, передбаченого теоретично та виміряного експериментально, пояснюється як прояв особливого вимушеного характеру ефекту Доплера, який реалізується експериментально при нерівноважних термодинамічних умовах, зумовлених дією лазерного випромінювання.
Ключові слова: термокапілярна пастка; газова бульбашка; розсіювання лазерного світла; інтерференційна картина; показник заломлення; ефект Доплера.

Продемонстрирована возможность контроля и управления размером газового пузырька, который находится в поглощающей свет жидкости и захвачен в лазерную термокапиллярную ловушку. Грубая структура интерференционных картин, которые наблюдаются в отраженном и пропущенном свете, объясняется качественно в рамках двухлучевого приближения. Движение интерференционных полос можно рассматривать как проявление эффекта Доплера на движущихся стенках пузырька. Предложен метод определения относительного показателя преломления двух смежных сред с движущейся границей раздела между ними посредством измерения отношения доплеровских сдвигов частот. Имеющееся двухкратное расхождение в значениях этого отношения, предсказываемого теоретически и измеренного экспериментально, объясняется как проявление особенного вынужденного характера эффекта Доплера, который реализуется экспериментально при неравновесных термодинамических условиях, обусловленных действием лазерного излучения.
Ключевые слова: термокапиллярная ловушка; газовый пузырек; рассеяние лазерного света; интерференционная картина; показатель преломления; эффект Доплера.

Introduction

Light fields are subjected to substance distribution for the most of the well-known classical optical phenomena in nature, but soon afterwards laser invention and, especially, after particles laser trapping experiments, it became clear that alternative contrary situations are possible up to and including Bose-Einstein condensation. Microparticles with relative refractive index $n>1$ are trapped easily by means of known Ashkin's dipole force technique. To trap particles with $n<1$, e.g. gas bubbles in liquid, it becomes rather more involved [1]. But because of surface tension temperature dependence it is possible to trap the gas bubble easily using so-called dissipative thermo-capillary force in the absorbing liquids [2, 3]. A broad size range of the bubbles, captured by a light beam, a large action radius and a high specific value of the capturing force are some of the useful thermo-capillary trap properties [4]. In the process they are evidently adjustable varying with the liquid medium absorbance. It is believed our results also can be regarded as an increasing appeal of the optical thermo-capillary gas

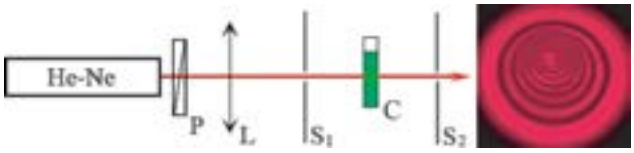

Fig. 1. Principal experimental scheme of the laser thermocapillary trap: **He-Ne** – laser used; **P** – linear polarizer; **L** – convergent lens; **C**– cell with an absorbing liquid; **S1** and **S2** – plane screens. Photo inset shows observed on screen **S2** pattern of Gaussian laser beam thermal self-defocusing.

bubble trap technique.

Experimental scheme and results

Our experimental setup is extremely simple (Fig. 1). A linearly polarised laser beam is focused on the cell C, containing an absorbing liquid, by means of the converging lens L. The cell is arranged between the screens S_1 and S_2 to observe the interference patterns (see lower) in reflected (RL) and transmitted light (TL). The polarizer P is used to control the laser beam power. There is some degree of freedom in the choice of laser types and liquids, but, evidently, laser light wavelength has to fall into the absorption band of the liquid. He-Ne-laser at λ = 632.8 nm and power P ≈ 15 mW jointly with ethanol solution, coloured by brilliant green dye, has been applied in our experiments. The photo in Fig. 1 demonstrates thermal self-defocusing (thermal lens aberration) observed on the screen S_2, created by a focused Gaussian laser beam in the solution mentioned above. But if the gas bubble is captured by the beam [2], then interference patterns shown in photos of Fig. 2 are appearing sharply on the screens S_1 and S_2. The radii of circular interference fringes are increasing or decreasing with time obviously in the process of bubble size change. As a rule, at laser power P ≈ 10 mW, diameters of the interference circles grow if a gas bubble is trapped in a dense solution, and, on the contrary, they reduce if capturing takes place in a dilute solution. It is noticeable that this evolution process can be controlled by means of the linear polarizer P. The process of changing the size of captured gas bubble can be stopped by increasing or decreasing the laser beam power and directed toward gas bubble growth or collapse at will.

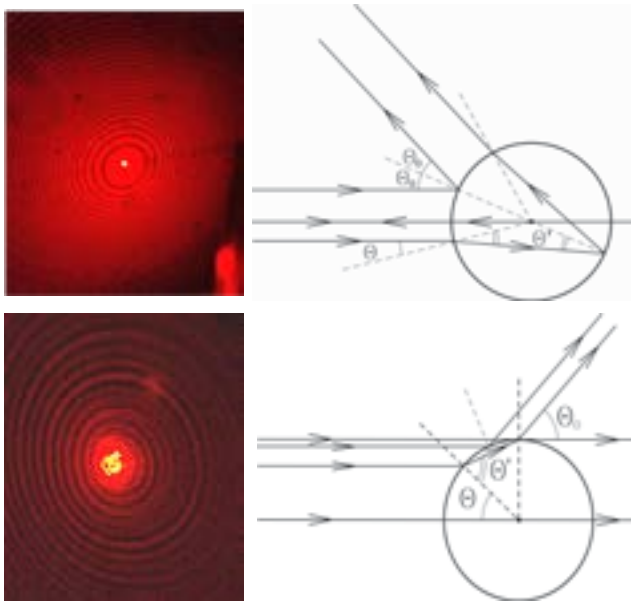

Fig. 2. The interference patterns observed on the screens **S1** in reflected (upper) and **S2** in transmitted (lower) lights after the gas bubble capture. The drawing schemes explain the patterns in an approach of two-ray interference: **Θ** and **Θ′** are angles of incidence and refraction on the gas bubble surface; $\mathbf{2\Theta_0}$ and $\mathbf{\Theta_0}$ are angles of deflections in reflected and transmitted lights.

Two-ray interference and Doppler effect

The interference pictures in the photos (Fig. 2) have both coarse (CFS) and fine fringe structures (only the CFS is noticeable in the photos). Certainly, Mie theory [5, 8] or generalized Lorenz-Mie theory [6] has to be applied to explain the structure completely. But one way of looking at the CFS is in terms of two-ray interference. Beam courses are sketched on the schemes in Fig. 2 at zero and maximum angles of deflection (n=1.360 is taken as the initial value for ethanol). If $2\Theta_0$ and Θ_0 are deflection angles in RL and TL accordingly, their magnitudes determine interference circles radiuses, Θ and Θ′ are angles of incidence and refraction on a bubble surface (Fig. 2), then the following correlations take place:

$$\theta_0 = 2\cdot\theta' - \theta \text{ in RL; } \theta_0 = 2\cdot(\theta' - \theta) \text{ in TL;}$$
$$\sin\theta' = n\cdot\sin\theta \quad .$$

In doing so, an optical path difference is arising in RL:

$$\Delta_r(\theta) = d\cdot\left(2\cdot\cos\theta' - n\cdot(\sin\theta_0 + \sin\theta)\cdot\tan(\theta' - \theta)\right). \quad (1)$$

And the same in TL:

$$\Delta_t(\theta) = d\cdot(\cos\theta' - n\cdot\cos\theta)\cdot(1 - \sin\theta'). \quad (2)$$

Here d is a bubble diameter. If this value is changing with time then, for a constant interference order, the values of deflection angles have to be changed both in RL and in TL. It clarifies the interference patterns movement. Let time derivatives be specified by primes. Then we have at the limit of zero deflection angles from (1) and (2):

$$\left|\Delta_r'(0)/\Delta_t'(0)\right| = 2/(n-1) = \left|\delta\omega_r/\delta\omega_t\right|. \quad (3)$$

In Eqn. (3) the last fraction is the ratio of Doppler frequency shifts for the waves reflected from ($\delta\omega_r$) and transmitted through ($\delta\omega_t$) the moving dielectric interface [7]. Hence observed interference patterns time evolution can be treated as a manifestation of the Doppler effect on the moving bubble walls. Measurement of the Doppler shifts ratio (DSR) gives the method to determine the

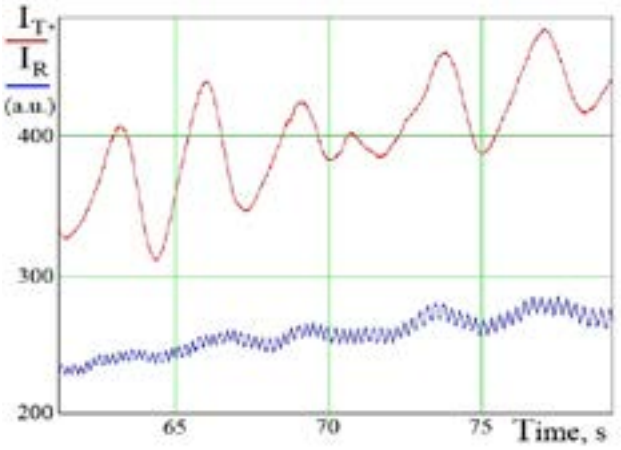

Fig. 3. The time dependences of the transmitted $\mathbf{I_T}$ (upper red) and reflected $\mathbf{I_R}$ (lower blue) signals at moving interference patterns of Fig. 2; the observation angle ($n\cdot\Theta_0$ for $\mathbf{I_T}$ and $2\cdot n\cdot\Theta_0$ for $\mathbf{I_R}$) is equal to 1/15 rad. The experimental value of Doppler frequency shifts ratio is $\delta\omega_r / \delta\omega_t \approx 71/6$.

refractive index n value in the vicinity of the bubble.

To carry out the measurement, optical fibers were arranged instead of the screens S_1 and S_2 (Fig. 1). Reflected and transmitted signals were communicated by means of the fibers to photomultipliers and further to computer after an analogue-digital transformation. One of the measurement results is displayed in Fig. 3. The transmitted signal I_T is sketched by the upper red curve, the reflected I_R – by the lower blue.

In doing so the angle of observation ($n\cdot\Theta_0$ for I_T and $2\cdot n\cdot\Theta_0$ for I_R) was ~1/15 rad. According to (3) at initial value n=1.360 the DSR has to be equal about six, while from Fig. 3 it results in 71/6, i.e. close to twelve.

At first glance, this two-times disagreement is naturally connected with a rough estimate of our two-ray interference model. To elucidate the question the MiePlot-4503 program [8] was applied to the problem of a plane wave scattering on the gas bubble surrounded by ethanol. At reasonably small deflection angles in RL and TL the program gives the DSR value about 63/10, which is in a satisfactory correspondence with Eqn. (3). Therefore, both Mie theory, and two-ray interference model results in the same DSR. Another source of the discrepancy could be caused by the motion of the gas bubble centre in the process of a bubble growth or collapse [9]. But a more attentive examination of this item testifies to the validity of Eqn. (3): a displacement of the bubble as a whole has no influence on the optical path differences $\Delta_r(0)$ and $\Delta_t(0)$ in the RL and TL accordingly.

Stimulated Doppler effect

From the above discussion it follows that the theoretical approaches do not take into account one essential feature of the experiment – the movement of gas bubble walls is stimulated by the laser light. At the limit of zero deflection angles the Doppler effect takes place on the moving back bubble surface only, both in RL and TL, because the front bubble wall is constantly in contact with an immobile wall of the cell [2]. Let a photon of the laser light be an incident on some small-scale area of the back bubble wall

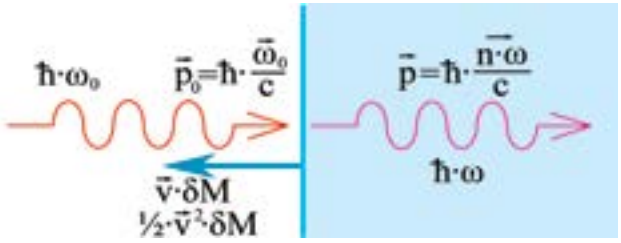

Fig. 4. A photon of the laser light is an incident on some small-scale area of the back moving bubble wall: ω_0 and ω are the frequencies of the photons incident on and passed through the surface accordingly; n is the refractive index of the liquid; $\vec{v}$ is the velocity of the moving interface.

(Fig. 4). If δM is some mass, connected with that area (the sense of δM will be adjusted later on), then the following impulse-energy conservation laws have to be fulfilled:

$$\vec{\mathbf{p}}_0 = \vec{\mathbf{p}} + \vec{\mathbf{v}}\cdot\delta M; \tag{4}$$

$$\hbar\cdot\omega_0 = \hbar\cdot\omega + \mathbf{v}^2\cdot\delta M/2. \tag{5}$$

Here $\left(\vec{\mathbf{p}}_0,\ \hbar\cdot\omega_0\right)$ is an impulse-energy of the incident photon; $\left(\vec{\mathbf{p}},\ \hbar\cdot\omega\right)$ is the same of the transmitted one; $\left(\vec{\mathbf{v}}\cdot\delta M,\ \mathbf{v}^2\cdot\delta M/2\right)$ is the same of the mass δM. Assuming $\omega \approx \omega_0$ and in the collinear geometry, as it is shown in Fig. 4, we have:

$$\delta M \approx \pm\frac{\hbar\cdot\omega_0}{\mathbf{v}\cdot c}\cdot(n-1); \tag{6}$$

$$\delta\omega_t = \omega - \omega_0 \approx \mp\frac{(n-1)\cdot\mathbf{v}}{2\cdot c}\cdot\omega_0. \tag{7}$$

In Eqns. (6, 7) the upper sign corresponds to the counter movement of the incident wave and the interface (as in Fig. 4), the lower sign – to their passing movement. Perhaps, the δM could be named, to some extent, as a "mass defect" of the treated small-scale area in the process of photon transition through the surface, the movement of which is stimulated by that transition. In our case this "mass defect" has rather a classical, non-relativistic nature: if δM is a positive, then a gas condensation process is occurring into the liquid; at opposite condition the liquid evaporation into the gas phase is preferred. The condensation-evaporation processes are controlled in our experiment by means of the laser light intensity value and it is possible because non-

equilibrium thermodynamic conditions, created by the laser beam, have realized in our system.

Eqns. (6) and (7) describe stimulated Doppler effect (SDE) at the collinear geometry in TL. The well-known substitution of the refractive index n value on minus unity [10] in these equations leads to the formulas, which deal with the SDE at the collinear geometry in RL:

$$\delta M \approx \mp \frac{2 \cdot \hbar \cdot \omega_0}{\mathbf{v} \cdot c}; \tag{8}$$

$$\delta\omega_r = \omega - \omega_0 \approx \pm \frac{\mathbf{v}}{c} \cdot \omega_0. \tag{9}$$

Certainly, Eqns. (6) - (9) corresponds to the particular cases of the more general non-collinear SDE. From Eqns. (4) and (5) it is straightforward to deduce the extended relations for the SDE "mass defect" δM and Doppler shift δω:

$$\delta M \approx -\frac{\hbar}{\mathbf{v}^2} \cdot \vec{\mathbf{v}} \cdot \delta\vec{\mathbf{k}}; \tag{10}$$

$$\delta\omega = \omega - \omega_0 \approx \frac{1}{2} \cdot \vec{\mathbf{v}} \cdot \delta\vec{\mathbf{k}}, \tag{11}$$

where $\delta\vec{\mathbf{k}} = \vec{\mathbf{k}} - \vec{\mathbf{k}}_{\mathbf{0}}$ is the wave vector change in the process assuming $\omega \approx \omega_0$.

Eqns. (6), (8) or (10) points out the fact that the process of interface movement should be consistent with the process of mass release or deposition. In contrast to the classical Doppler effect (CDE), the SDE is not possible simultaneously in transition and reflection on the same portion of the surface because of the different signs and values of δM in RL and TL. If the SDE takes place at small deflection angles in transmition, then the CDE should be observed at the same angles in reflection or vice versa. We suppose it is the former that has been realized in our experiment. Doppler frequency shifts at the CDE are two times greater than the corresponding SDE shifts, $\delta\omega_t$, $\delta\omega_r$ or δω in Eqns. (7), (9) or (11). Then the DSR $\delta\omega_r/\delta\omega_r$ value ought to be double of the result of Eqn. (3), if the CDE is present in RL and the SDE – in TL. Finally, it is necessary to note, that at a non-stimulated nature of the gas bubble growth or collapse it is the classical DSR value of Eqn. (3) that should be observed in experiments, since only the CDE should take place on the bubble walls.

Summary

As it has been mentioned above, laser beam thermal self-defocusing is observed in our experiment. It indicates of the noticeable optical nonlinearity of the used liquid. The measurement of the DSR gives a possibility to determine the refractive index value n including a nonlinear optics contribution. Therefore, at the limit of zero deflection angles we have:

$$\frac{\delta\omega_r}{\delta\omega_t} = \frac{4}{n-1} \approx \frac{71}{6}. \tag{12}$$

Calculated by Eqn. (12) value $n \approx 1.338$ is much better than by using Eqn. (3). But we have to take into account that our measurements were carried out at the non-zero observation (deflection) angles. Under the assumption that the SDE takes place as well at the total internal reflection on the bubble periphery, it follows from Eqn. (11) the linear angle correction to the DSR is equal to $2n \cdot \theta_0/(n-1)^2$, here $n \cdot \theta_0$ is the observation angle in TL, its magnitude is equal to 1/15 rad. An approximately half of that value is accounted for the angle half-width of the self-defocusing pattern shown in the photo-inset of Fig. 1. That is why we suppose that only the half of the angle correction written above is suitable to correct the DSR value:

$$\frac{4}{n-1} + \frac{n \cdot \theta_0}{(n-1)^2} \approx \frac{71}{6}. \tag{13}$$

Last equation results in $n \approx 1.3539$. It is the latter value that we consider as final and therefore the refractive index variation $\Delta n \approx 0.006$ is caused by the thermal optical nonlinearity. These results are in sufficiently well accordance with the experimental estimations obtained in the earlier research [2, 9].

In conclusion, the refractive index determination by means of the DSR measurements is well suited method for optical applications, especially in the field of nonlinear optics.

Acknowledgment

V. I. L. would like to express a sincere gratitude to Prof. Philip Laven for his remarkably helpful Internet site [8] and, especially, for his kind permission to use the program MiePlot-4503 and its results for the report. To the light memory of V.K. Miloslavsky.

References

1. Lankers M., Khaled E.E.M., Popp J., Rossling G., Stahl H., and Kiefer W., Determination of size changes of optically trapped gas bubbles by elastic light backscattering, Appl. Opt., vol. 36, No.7, pp.1638-1643, 1997.
2. Yarovaya R.G., Makarovskii N.A., and Lupashko N.A., Influence of a laser beam on the motion of gas bubbles in an absorbing liquid, Sov. Journ. Tech. Phys., vol. 33, No.7, pp. 817-821, 1988.
3. Bazhenov V.Yu., Vasnetsov M.V., Soskin M.S., and Taranenko V.B., Dynamics of laser-induced bubble and free-surface oscillations in an absorbing liquid, Appl. Phys. B, vol. B49, pp. 485-489, 1989.
4. Ivanova N.A., Bezugliy B.A., Optical thermocapillary trap for a bubble, Pis'ma Zhurn. Tekhn. Fiz., vol. 32, No.19, pp. 66-71, 2006. *(in Russian)*.
5. C.F. Bohren, and D.R. Huffman, Absorption and scattering of light by small particles (Wiley, New-York, 1983).
6. G. Gouesbet, G. Grehan, Generalized Lorenz-Mie theories (Springer-Verlag, Berlin-Heidelberg, 2011).
7. I. Ye. Tamm, Foundations of electricity theory (Nauka, Moscow, 1989). *(in Russian)*.
8. See, please, the internet site "The Optics of a Water Drop (Mie Scattering and the Debye Series)" by Prof. Philip Laven: http://www.philiplaven.com/ index1.html; http://www.philiplaven.com/mieplot.htm/.
9. A.D. Butenko, N.A. Kazachkova, O.I. Kofman and V.I. Lymar, "Optical gas bubble management" at its laser thermo-capillary trapping in an absorbing liquid, ME-21 in Proceedings of the 10th Int. Conf. on Laser-light and Interactions with Particles, F. Onofri and B. Stout, eds., Aix-Marseille University, Marseille, August 2014.
10. R.P.Feynman, R.B. Leighton, M. Sands, The Feynman lectures on physics (Addisson-Wesley Pub. Co., Reading-London, 1963).